



Published in final edited form as:

*Nanotoxicology*. 2016 March ; 10(2): 140–150. doi:10.3109/17435390.2015.1025115.

## Short-term exposure to engineered nanomaterials affects cellular epigenome

Xiaoyan Lu<sup>1</sup>, Isabelle R. Miousse<sup>2</sup>, Sandra V. Pirela<sup>1</sup>, Stepan Melnyk<sup>3</sup>, Igor Koturbash<sup>2,\*</sup>, and Philip Demokritou<sup>1,\*</sup>

<sup>1</sup>Center for Nanotechnology and Nanotoxicology, Department of Environmental Health, Harvard School of Public Health, Boston, MA, USA

<sup>2</sup>Department of Environmental and Occupational Health, College of Public Health, University of Arkansas for Medical Sciences, Little Rock, AR, USA

<sup>3</sup>Department of Pediatrics, University of Arkansas for Medical Sciences, Little Rock, AR, USA

### Abstract

Extensive incorporation of engineered nanomaterials (ENMs) into industrial and biomedical applications increases the risks of exposure to these potentially hazardous materials. While the geno- and cytotoxic effects of ENMs have been investigated, the potential of ENMs to target the cellular epigenome remains largely unknown. Our goal was to determine whether or not industry relevant ENMs can affect the epigenome at low cytotoxic doses. A panel of cells relevant to inhalation exposures such as human and murine macrophages (THP-1 and RAW264.7, respectively) and human small airway epithelial cells (SAEC) were exposed to printer-emitted engineered nanoparticles (PEPs), mild steel welding fumes (MS-WF), copper oxide (CuO), and titanium dioxide (TiO<sub>2</sub>) nanoparticles. Toxicological effects, including cytotoxicity, oxidative stress, and inflammatory responses were assessed, taking into consideration in-vitro dosimetry. The effects of ENMs on cellular epigenome were determined by addressing the global and transposable elements (TEs)-associated DNA methylation and expression of DNA methylation machinery and TEs. The percentage of ENMs-induced cytotoxicity for all cell lines was in the range of 0–15%. Oxidative stress was evident in SAEC after exposure to PEPs and in THP-1 when exposed to CuO. Additionally, exposure to ENMs resulted in modest alterations in DNA methylation of two most abundant TEs in mammalian genomes, LINE-1 and *Alu*/SINE, their transcriptional reactivation, and decreased expression of DNA methylation machinery in a cell-, dose-, and ENM-dependent manner. These results indicate that exposure to ENMs at environmentally relevant concentrations, aside from the geno- and cytotoxic effects, can also affect the epigenome of target cells.

\*Corresponding authors: Philip Demokritou, Department of Environmental Health, Harvard School of Public Health, Harvard University, 665 Huntington Avenue, Boston, MA 02115, USA. Tel: +1 6174323481. pdemokri@hsph.harvard.edu; Igor Koturbash, Department of Environmental and Occupational Health, College of Public Health, University of Arkansas for Medical Sciences, Little Rock, AR, 72205, USA. Tel: +1 5015266638. IKoturbash@uams.edu.

**Declaration of interests:** The authors report no competing financial interests. The authors alone are responsible for the content and writing of the paper.

## Keywords

Engineered nanomaterials; epigenetics; printer-emitted particles; DNA methylation; transposable elements

---

## Introduction

Due to their unique physicochemical and mechanical properties, ENMs are used extensively in many industrial products and biomedical applications (Pirela et al., 2014b; Pyrgiotakis et al., 2014). While the geno- and cytotoxic effects of ENMs have been investigated in many studies (Cohen et al., 2014a; Setyawati et al., 2013; Sotiriou et al., 2014; Watson et al., 2014), the potential of ENMs to target the cellular epigenome remains largely unknown. However, it is becoming increasingly recognized that environmental stressors can affect epigenetic mechanisms and that these alterations can play a key role in the development and progression of diseases (Bollati and Baccarelli 2010; Koturbash et al., 2011a).

Epigenetics define somatically heritable changes in gene expression without alterations in DNA sequence. Epigenetic mechanisms of regulation include methylation of DNA, histone modifications, regulation by non-coding RNAs, and nucleosome positioning. DNA methylation, the most studied epigenetic event, plays a critical role during the development and maintenance of cellular homeostasis. It regulates the expression of genetic information in a sex-, tissue-, and cell type-dependent manner and serves as a key mechanism in silencing of TEs (reviewed in Jones 2012).

Environmental factors have been reported to target the cellular epigenome, indicating TEs as one of the primary targets for alterations in DNA methylation. This is largely due to their abundance: up to two thirds of the genome is estimated to be comprised by TEs (de Koning et al., 2011). A wealth of studies have concluded that ambient particulate matter (PM<sub>2.5</sub> and PM<sub>10</sub>) can induce hypomethylation of TEs in blood/buccal cells of exposed humans and in animal and in-vitro models (Baccarelli et al., 2009; Madrigano et al., 2011; Miousse et al., 2014a; Salam et al., 2012; Stoccoro et al., 2013; Tarantini et al., 2009).

Limited but increasing evidence clearly points to the ability of ENMs to induce epigenetic changes. For instance, cadmium telluride quantum dots (CdTe QDs) have been shown to induce histone hypoacetylation in human breast carcinoma cells (Choi et al., 2008). Other ENMs, such as gold nanoparticles, iron (III) oxide nanoparticles, multi-walled carbon nanotubes, and CdTe QDs induced alterations in miRNA expression (Li et al., 2011; Ng et al., 2011). Similarly, microRNAome was affected in in-vivo studies (Balansky et al., 2013; Halappanavar et al., 2011). Of particular interest is the study by Gong et al. (2010), reporting that the short-term (24 h) treatment of human keratinocyte cells (HaCaT) with nano-silicon dioxide induced dose-dependent global genomic hypomethylation and alterations in DNA methylation machinery.

Here we hypothesize that ENMs may cause epigenetic changes, exhibited as 1) alterations in global and TEs-associated DNA methylation and 2) the expression of TEs and DNA methylation machinery and that these alterations are both cell- and ENM-dependent. Taking

into account that alveolar epithelial cells and macrophages are directly in contact with inhaled particles and constitute the first line of defense against foreign particles in the lung (Hiraiwa and van Eeden 2013), we exposed these cells to a number of industry related ENMs: PEPs, MS-WF, CuO, and TiO<sub>2</sub> nanoparticles at low cytotoxic dose levels. The overall research strategy and experimental design for the study is outlined in Figure 1.

## Methods

### Sources and Characterization of ENMs

A variety of ENMs widely used in commercial applications (TiO<sub>2</sub>, CuO) as well as engineered nanoparticles released in the air from nano-enabled products during consumer use (PEPs) and nanoparticles of known toxicological and chemical footprint (MS-WF) were used in the study. The MS-WF particles were a kind gift from Dr. James M Antonini from the National Institute for Occupational Safety and Health and their physico-chemical properties are described in detail in a previous study (Zeidler-Erdely et al., 2010). The PEPs were sampled using a newly developed printer exposure generation systems described in our previous publication (Pirela et al., 2014a). The TiO<sub>2</sub> and CuO were commercially obtained from EVONIK (EVONIK, Parsippany, NJ) and Sigma Aldrich (Sigma, St. Louis, MO), respectively.

The specific surface area (SSA, m<sup>2</sup>/g) of MS-WF, TiO<sub>2</sub>, and CuO was measured by the nitrogen adsorption/Brunauer-Emmett-Teller (BET) method using a Micrometrics Tristar 3000 (Micrometrics, Inc., Norcross, GA). The average primary particle diameter  $d_{BET}$  of these ENMs was determined from their SSA as  $d_{BET} \text{ (nm)} = 6000/(\rho \times \text{SSA})$ , where  $\rho$  is the material density. Morphological assessment was subsequently performed using transmission electron microscopy (TEM) by a JEOL2100 microscope (JEOL, Peabody, MA) as described in great detail on a previous study (Sotiriou et al., 2012). The detailed chemical composition of PEPs which were collected from printer B1 is described in our previous study (Pirela et al., 2014b). Only PEPs with an aerodynamic diameter smaller than 0.1  $\mu\text{m}$  (PM<sub>0.1</sub>) were used in this study.

### ENM dispersal and characterization in liquid suspensions

The critical delivered sonication energy (DSEcr) of the ENMs was determined in order to break powder agglomerates in deionized water (DI H<sub>2</sub>O) and achieve stable monodispersed agglomerates based on a previously established protocol (Cohen et al., 2013). The DSEcr of MS-WF, TiO<sub>2</sub>, CuO, and PEPs was found to be 400, 161, 242, and 514 J/mL, respectively.

The preparation and characterization of particle suspensions for the toxicological studies was performed as follows: a 1 mg/mL stock suspension of each particle suspended in DI H<sub>2</sub>O was sonicated to the DSEcr using a Branson Sonifier S-450A (Branson Ultrasonics, Danbury, CT). The DI H<sub>2</sub>O-particle suspensions were then diluted to 100  $\mu\text{g/mL}$  level using the appropriate type of cellular media for the various cell lines used in the study: small airway epithelial cell growth medium with the SAGM bullet kit (SAGM, LONZA, Allendale, NJ) for SAEC, Roswell Park Memorial Institute (RPMI) supplemented with 10% heat-inactivated fetal bovine serum (FBS) and 1 $\times$ Antibiotic-Antimycotic (RPMI/10%FBS)

for THP-1, and Dulbecco's Modified Eagle Medium (DMEM) supplemented with 10% FBS and 100 U/mL penicillin-streptomycin (DMEM/10%FBS) for RAW264.7 (Life Technologies, Grand Island, NY). The pH of all the three media was 7.4. The hydrodynamic diameter ( $d_H$ ), polydispersity index (PdI), zeta potential ( $\zeta$ ), and specific conductance ( $\sigma$ ) of these dispersions at 0 and 24 h exposure time were analyzed by dynamic light scattering (DLS) (ZetasizerNano-ZS, Malvern Instruments, Worcestershire, UK). In addition, the effective density of the formed ENM agglomerates in the culture media was determined using the volumetric centrifugation method (VCM) recently developed by our group (DeLoid et al., 2014). Effective density along with the size of the formed agglomerates are the two most important determinants of the fate and transport and dosimetry in-vitro (Cohen et al., 2014b). A brief description of the VCM method is presented in Supplementary Materials.

### **In-vitro dosimetric considerations**

The actual delivered-to-cell dose of the test particles in specific media as a function of exposure time was determined by the hybrid VCM-in-vitro sedimentation, diffusion, and dosimetry (VCM-ISDD) method recently developed by our group (Cohen et al., 2014b; Deloid et al., 2014). A brief description is presented in Supplementary Materials.

### **Cell culture**

The RAW264.7 were purchased from ATCC (Manassas, VA) and cultured in DMEM/10% FBS. The SAEC were a present from Jennifer Sisler (NIOSH, Morgantown, WV) and cultured in SAGM. The THP-1 were a gift from Dr. Lester Kobzik (Harvard School of Public Health, Boston, MA) and cultured in RPMI/10% FBS. All cells were cultured at 37°C with 5% carbon dioxide.

The cells were exposed to MS-WF, TiO<sub>2</sub>, CuO, and PEPs dispersed in the respective cell culture media at two doses (0.5 and 30 µg/mL) for 24 h. PEPs exposures were only performed on the SAEC and RAW264.7, while the three other particle types were used on all three cell lines. All ENM suspensions were prepared as described above prior to cellular treatment. Cell seeding and harvesting details can found in Supplementary Materials.

### **Cell viability analysis**

The CytoTox-One Homegenous Membrane Integrity Assay (Promega, Madison, WI) was used to estimate the number of non-viable cells present after the exposure to ENMs by measuring the amount of lactate dehydrogenase (LDH) leaked from the cells. The Lysis Solution was used as a positive control, which was included in CytoTox-One Homegenous Membrane Integrity Assay to generate maximum LDH release. Fluorescence intensity was detected by SoftMax Pro 6 GxP Microplate Data Acquisition and Analysis System (Molecular Devices, Sunnyvale, CA) with an excitation/emission wavelength of 560/590 nm. To ensure that the nanoparticles did not interfere with the assay results, particle-only and media-only control groups were used. The particle-only controls were particles in media at 0.5 or 30 µg/ml concentrations (without cells), and media-only controls were only media in the absence of cells. Results indicated that the fluorescence intensity of the particle-only

control groups was almost the same as the media-only group indicative of no autofluorescence effects from particles (data not shown).

### **Oxidative stress assessment**

Dihydroethidium (DHE), a superoxide indicator, is a fluorescent probe used to evaluate the oxidative stress in cells after exposure to ENMs. Fifteen percent hydrogen peroxide (15% H<sub>2</sub>O<sub>2</sub>, 4.9 mol/L) was used as positive control for 30 min at the end of 24 h exposure. Then, cells were incubated with 5 µM DHE at 37°C for 30 min. The fluorescence intensity was detected by SoftMax Pro 6 GxP Microplate Data Acquisition and Analysis System (Molecular Devices, Sunnyvale, CA) with an excitation/emission wavelength of 518/605 nm. Particle-only control experiments were also included in this assay and compared with media-only control groups. Results indicated that autofluorescence effects were only detected in the particle-only control groups of MS-WF and TiO<sub>2</sub> in SAEC media and TiO<sub>2</sub> in THP-1 media at 30 µg/mL. Thus, the signals for the aforementioned ENM exposures in both cell lines were corrected to take into the account the autofluorescence effects of particle-only controls.

### **Cytokines analysis**

SAEC were treated with 30 µg/mL MS-WF, CuO, and PEPs for 24 h. Cell supernatants were collected and assayed by Eve technologies using a human 41-multiplex assay (Eve Technologies, Calgary, Alberta, Canada). The standard curve matrix which is the equivalent of a positive control is used by EVE Technologies with their own specific standard samples for each cytokine (Bedran et al., 2014; Egli et al., 2014).

### **Nucleic Acids Extraction**

RNA and DNA were extracted simultaneously from flash-frozen cells using the AllPrep Mini Kit (Qiagen, Valencia, CA) according to the manufacturer's protocol. DNA concentrations were analyzed by the Nanodrop 2000 (Thermo Scientific, Waltham, MA), and DNA integrity was evaluated on 1% agarose gel.

### **Analysis of 5-Methylcytosine (5-mC) and 5-hydroxymethylcytosine (5-hmC) levels**

RNaseA (Sigma, St. Louis, MO) was added to 1 µg of genomic DNA to a final concentration of 0.02 mg/mL and incubated at 37°C for 15 min. Purified DNA was digested into component nucleotides using Nuclease P1, snake venom phosphodiesterase, and alkaline phosphatase as previously described (James et al., 2010). Methodology has been described in Supplementary Materials.

### **Analysis of methylation status of TEs**

Methylation at the LINE1 and *Alu*/SINE elements was assessed by methylation-sensitive quantitative Real-Time Polymerase Chain Reaction (qRT-PCR). The detail method has been described in Supplementary Materials. Primers are listed in Supplementary Table 1.

## Quantitative analysis of gene and TEs expression levels

Complementary DNA (cDNA) was synthesized from 1 µg RNA using random primers and a High Capacity cDNA Reverse Transcription Kit (Applied Biosystems, Foster City, CA) according to the manufacturer's protocol. Quantitative real-time PCR (qRT-PCR) to determine the levels of gene transcripts was performed using 10 ng of cDNA per reaction and the TaqMan Universal PCR Master Mix, no AmpErase® UNG (Life Technologies) on a ViiA 7 instrument (Life Technologies). Assay IDs used in the study are provided in Supplementary Table 2. Primers for determination of mRNA abundance of LINE-1 and *Alu*/SINE elements are provided in the Supplementary Table 3. The  $C_t$  values for all genes were determined relative to the control gene *GAPDH* or *RPS13/Rps29* (Supplementary Tables 2 and 3). The  $C_t$  were calculated using each exposed group means relative to control group as described previously (Schmittgen and Livak, 2008). All qRT-PCR reactions were conducted in triplicate and repeated twice.

## Copy numbers analysis

LINE-1 copy number was assessed as following: LINE1 ORF2 was amplified by real-time quantitative PCR from 10 ng of gDNA. Relative abundance of the target in gDNA was normalized to 5S ribosomal DNA using the  $C_t$  method. The FAM/ZEN-conjugated primers with the probe sequence are shown in Supplementary Table 4 (Integrated DNA Technologies, Coralville, IA) and were used at a final concentration of 5 µM. Amplification was performed for 40 cycles using conditions for the 2× Taqman Universal Master Mix as recommended by the manufacturer (Life Technologies).

## Statistical analysis

The significance was determined by one way ANOVA, followed by Dunnett's or Tukey's test using GraphPad Prism 5.0 software. A  $p$ -value  $\leq 0.05$  was considered to be significant.

## Results

### Physicochemical and morphological characterization of ENMs

Primary particle size as determined by BET and TEM methods for MS-WF, TiO<sub>2</sub>, CuO, or PEPs is shown in Supplementary Figure 1. The BET diameters for MS-WF, TiO<sub>2</sub>, and CuO were 23.8, 21.0, and 58.7 nm, respectively. Similar results were observed by TEM analysis. Moreover, the primary particle size of PEPs was also below 100 nm detected by TEM analysis.

Colloidal properties measured by DLS for all ENMs suspended at 100 µg/mL in either DI H<sub>2</sub>O or media are summarized in Supplementary Table 5. First, the  $d_H$  and zeta potential were measured at 0 h after sonication by DESr. Generally, formed ENM agglomerates in SAGM were bigger than other two media. As shown in suppl. Table 5, for MS-WF, TiO<sub>2</sub>, CuO, or PEPs in SAGM, the  $d_H$  was found to be  $1526.7 \pm 259.6$ ,  $774.4 \pm 59.61$ ,  $1367 \pm 73.12$ , and  $381.7 \pm 40.2$  nm, respectively. In RPMI/10%FBS, the  $d_H$  for TiO<sub>2</sub>, CuO, or PEPs was much smaller than that in SAGM and detected as  $307.7 \pm 25.22$ ,  $907.9 \pm 24.81$ , and  $227.3 \pm 105.0$  nm for these particles, respectively, with little change for MS-WF ( $1502 \pm 96.26$  nm). Similarly, the  $d_H$  for all ENMs in DMEM/10%FBS was also smaller than that in



SAGM. It was observed as  $783.0 \pm 21.26$ ,  $390.4 \pm 16.04$ ,  $828.3 \pm 95.49$ , and  $298.0 \pm 5.73$  nm for MS-WF, TiO<sub>2</sub>, CuO, or PEPs, respectively. Moreover, the zeta potential was found to be negative for TiO<sub>2</sub> and CuO suspended in DI H<sub>2</sub>O and the three different media at 0 h. For PEPs and MS-WF in DMEM/10%FBS, zeta potential was found to be negative (-15.9 mV for PEPs, and -12.5 mV for MS-WF) as well as PEPs in DI H<sub>2</sub>O (-20.6 mV), and the rest were positive for these two ENMs in different suspensions at 0 h.

The stability of the colloids was also subsequently evaluated 24 h post-sonication to DSEcr (Supplementary Table 5). The  $d_H$  at 24 h was found to be similar as those of 0 h for all the ENMs in the three different media. Moreover, the zeta potential at 24 h was also consistent with the results of 0 h for TiO<sub>2</sub> and CuO suspended in DI H<sub>2</sub>O and the three different media. For PEPs, the zeta potential at 24 h was similar to those of 0 h in the three different media, except in SAGM which was a little bit lower than that of 0 h (1.22 mV at 24 h versus 9.97 mV at 0 h). For MS-WF, the zeta potential in SAGM and RPMI/10%FBS was turned to negative at 24 h (-7.56 mV for SAGM, and -7.63 mV for RPMI/10%FBS) and positive at 0 h (18.8 mV for SAGM, and 12.1 mV for RPMI/10%FBS); however, the zeta potential in DMEM/10% FBS was similar between 0 and 24 h. Taken together, the ENM suspensions exhibited stability during the exposure time.

### In-vitro dosimetric considerations

In order to determine the cell-delivered dose of all ENMs in the three cell culture media as a function of exposure time, the VCM-ISDD method was used. In general, ENMs with greater values of hydrodynamic diameter and effective density in media may deposit faster than those with smaller values. As shown in Supplementary Figures 2 and 3, CuO and MS-WF deposited at a faster rate than TiO<sub>2</sub> and PEPs in the three media for both well plate configurations. This is consistent with their relatively large hydrodynamic diameters (Supplementary Table 5). It will take less than 5 h for all of the administered mass of MS-WF or CuO to deposit on the cells for both the 96-well plate and 100-mm diameter dish configurations. However, the opposite was observed for TiO<sub>2</sub> and PEPs, especially when suspended in RPMI/10%FBS and DMEM/10%FBS. In 96-well plates, only approximately 66% of the administrated dose of PEPs in RPMI/10%FBS will actually reach the bottom of the wells after 24 h exposure, while about 37% of the PEPs in DMEM/10%FBS will reach the bottom; and approximately 93% of the administrated dose of TiO<sub>2</sub> in these two media will actually deposit to the bottom. Although with 100-mm diameter dishes, almost 100% TiO<sub>2</sub> and PEPs deposited to the bottom after 24 h exposure; settling times were longer than those of MS-WF and CuO that also settled 100% at 24 h exposure time.

### Cytotoxicity of ENMs

In order to evaluate the potential impact of ENMs on lung tissue, human epithelial cells as well as human and murine macrophages were exposed to MS-WF, TiO<sub>2</sub>, CuO, and/or PEPs at 0.5 (low dose) and 30 µg/mL (high dose) for 24 h. LDH analysis provides evidence that all ENMs have a dose-dependent cytotoxic response in all three cell lines, with the exception of CuO on THP-1. The two CuO treatments in this cell line didn't show any cytotoxicity compared with control group, while CuO were the only toxic particles on RAW264.7 among

all the ENMs. The percentage of cytotoxicity was in the range of 0-15% for all ENMs in the three cell lines, when compared to the untreated control group (Figure 2A).

### Oxidative stress induced by ENMs

Levels of ROS were increased in PEPs-treated SAEC and CuO-treated THP-1 at high dose (Figure 2B). Although slight increases were observed, no significant difference was evident in total DHE fluorescence between other ENMs and control groups in all three exposed cell lines (Figure 2B). Furthermore, an increase in the expression levels of heme oxygenase 1 (*HO-1*) was detected in all three cell lines, indicative of cells conferred cytoprotection in numerous models of oxidative injury (Lee et al., 2014). As shown in Figure 2C, CuO at the 30 µg/mL dose significantly increased more than 20-fold of *HO-1* expression in both THP-1 and RAW264.7 compared to the control group. While upregulation was also observed in SAEC for CuO treatment, it did not reach significance. Interestingly, PEPs upregulated *HO-1* expression only in SAEC at the 30 µg/mL dose ( $p < 0.01$ ), whereas MS-WF markedly increased *HO-1* expression in both SAEC and RAW264.7 at same dosage (Figure 2C).

### Effects of ENM exposures on cytokines

Levels of cytokines were measured in SAEC post-exposure to ENMs at high dose. Cytokine release for TiO<sub>2</sub> was not included as TiO<sub>2</sub> was found less toxic compared to other ENMs in the panel (see results above). Exposure to PEPs and MS-WF led to significantly elevated levels of ten cytokines (Supplementary Figure 4). Particularly, granulocyte macrophage colony-stimulating factor (GM-CSF), fractalkine, growth regulated oncogene (GRO), interleukin 6 (IL-6), IL-8, and monocyte Chemoattractant Protein-1 (MCP-1) increased over 88-fold when compared with the control group. CuO exposure had no effects on these cytokines; however, the levels of basic fibroblast growth factor (FGF-2), platelet-derived growth factor-BB (PDGF-BB), and IL-7 increased, while that of epidermal growth factor (EGF) was decreased (Supplementary Figure 5).

### Analysis of global DNA methylation

Global DNA methylation was addressed by measuring the levels of 5-mC in control and exposed cells. No significant differences were identified in the levels of 5-mC in response to ENM exposure (Figure 3, Panel A). At the same time, some minor differences in 5-mC levels were observed between the cells exposed to various ENMs.

### Analysis of methylation status of repetitive elements

Previous studies indicate that analysis of global DNA methylation may mask the redistribution of methylation patterns between the different genomic loci, where the hypomethylation of one and hypermethylation of others may result in cumulatively unchanged levels of DNA methylation (Miousse et al., 2014a). To further investigate whether this phenomenon can be associated with exposure to ENM, we evaluated the methylation status of two most abundant in human and mouse genomes TEs, LINE-1 (L1), and *Alu* elements that correspond to SINE B1 and SINE B2 in mouse.



First, we addressed the methylation status of L1 element in its four functional units: 5'- and 3'-untranslated regions (UTR) and two open reading frames (ORF1 and ORF2, Figure 4). We identified the hypomethylation of ORF1 in SAEC cells after exposure to higher dose of PEPs (30% decrease,  $p=0.04$ ). Interestingly, trends towards modest hypomethylation were also identified in ORF2 and 3'-UTR after exposure of SAEC to 30  $\mu\text{g/mL}$  of PEPs as well as the above mentioned decrease in 5-mC; however, they were statistically insignificant. Some statistically significant, although of very minor magnitude, hypermethylation effects were observed in 5'-UTR, ORF1, and ORF2 of SAEC in response to exposure to CuO. The same effects were detected in ORF2 of THP-1 after exposure to CuO at high dose. Weak hypomethylation was also identified in 5'-UTR and 3'-UTR of RAW264.7 after low dose CuO treatment.

We next addressed the methylation status of SINE B1 and SINE B2 (RAW264.7) and *Alu* elements (THP-1 and SAEC) after exposure to ENMs. Similar to effects observed in L1 5'-UTR, ORF1, and ORF2, significant hypermethylation of *Alu* elements in SAEC after exposure to higher dose of CuO was detected. Interestingly, a similar pattern was observed in THP-1, where exposure to both doses of CuO resulted in *Alu* hypermethylation. However, the most interesting results were found in RAW264.7, where exposure to virtually all ENMs resulted in modest hypermethylation of SINE B1 elements. No significant changes, although, were identified in methylation of SINE B2.

### Expression of transposable elements

Exposure to environmental stressors frequently results in transcriptional activation of TEs (Koturbash et al., 2011b; Miousse et al., 2014b; Rudin and Thompson 2001). Therefore, next we sought to evaluate the expression of L1 and *Alu*/SINE in response to exposure to ENMs (Figure 5). Exposure to a lower dose of  $\text{TiO}_2$  and both doses of CuO resulted in significant and profound reactivation of both L1 ORFs – ORF1 and ORF2 as well as SINE B1 and SINE B2 in RAW264.7. In contrast, exposure to a higher dose of MS-WF led to transcriptional activation of L1 ORF1 and ORF2 and *Alu* (although, the latter two – insignificant) in THP-1, while some weak L1 reactivation was also observed after exposure to a higher dose of  $\text{TiO}_2$ . Similar to THP-1, effects were detected in SAEC cells, where exposure to high dose of MS-WF and  $\text{TiO}_2$  resulted in increased transcripts of L1 ORF2 and *Alu* (although *Alu* in  $\text{TiO}_2$  treatment – insignificant). Additionally, exposure to higher dose PEPs also led to increased expression of *Alu* in SAEC.

### Analysis of L1 copy numbers

Reactivation of TEs, such as L1 and *Alu*/SINE, may lead to their retrotransposition and, subsequently, increase in their copy numbers. Taking into account the observed overexpression of L1 ORFs in response to ENMs, we addressed copy numbers of this highly abundant TE 24 h after exposure; however, we did not identify any significant increases in any of the treatment groups (Supplementary Figure 6).

### Exposure to ENMs and DNA methylation machinery

Identified changes in expression of genes may predict further alterations within the pathways they control. Therefore, next we addressed the expression of a panel of genes

directly involved in establishment and maintenance of methylation marks and, therefore, called DNA methylation machinery. The expression of *DNMT1*, DNA methyltransferase responsible for copying the methylation patterns during the replication on the newly synthesized DNA strand, was found to be negatively affected by exposure to high dose of all ENMs and in all tested cell lines. The only exception was found in SAEC after exposure to high dose of CuO, where a statistically significant ( $p=0.001$ ) 2-fold increase in the expression of *DNMT1* was observed. Similar patterns, however, less pronounced were observed for both *de novo* methyltransferases *DNMT3A* and *DNMT3B* as well as *UHRF1* (Figure 6).

### Effects of exposure to ENMs on DNA hydroxymethylation

Hydroxymethylation of DNA, an epigenetic mechanism discovered several years ago, is considered to be an intermediate chain in the process of DNA demethylation (Kohli and Zhang 2013). The levels of DNA hydroxymethylation in regard to exposure to ENMs were addressed by measuring the 5-hmC. Similar to 5-mC, exposure to ENMs did not greatly affect the levels of 5-hmC in any of the treatment groups, except the low dose MS-WF exposure in RAW264.7 (Figure 3, Panel B). In contrast to DNA methyltransferases, where the congruent response was found for all three genes (*DNMT1*, *DNMT3A*, and *DNMT3B*), *TET1-TET3* genes were differentially regulated, depending on the cell line, ENM, and dose. For instance, exposure to high dose of TiO<sub>2</sub> and PEPs resulted in increased expression of *Tet2* in RAW264.7, while high dose of MS-WF and CuO led to decreased mRNA levels of *Tet3* in the same cell line (Supplementary Figure 7). More simultaneous response was observed in SAEC, where high doses of MS-WF, TiO<sub>2</sub>, and CuO and both concentrations of PEPs resulted in decreased expression of all three methyl deoxyases.

### Discussion

In this study, it was demonstrated that ENMs at environmentally relevant concentrations and at low cytotoxicity levels, aside from the inflammatory response and oxidative stress, has also resulted in epigenetic alterations in the target cells – macrophages and lung epithelium. These effects were exhibited as alterations in methylation of two most abundant in mammalian genomes TEs – L1 and Alu/SINE, their reactivation, and down-regulation of DNA methylation machinery.

These epigenetic alterations were associated with minimal cytotoxic effects. The treatment doses of 0.5 and 30 µg/mL used were chosen to cause no more than 20% of cytotoxicity following exposure to the test materials used here. It is worth noting that for the case of PEPs that we have “real world” exposure data, the cell-administered doses of 0.5 and 30 µg/mL correspond to 1 and 60 h of inhalation exposure to PEPs emitted from laser printers (manuscript in preparation). As the results, the percentage of ENMs-induced cytotoxicity for all three cell lines was below 15%, and no significant changes were detected in cells exposed to 0.5 µg/mL of any of the ENMs. These data are in a good agreement with the previous studies (Badding et al., 2014; Sisler et al., 2014; Xia et al., 2013; Xiong et al., 2013).

Additionally, exposure to ENMs resulted in inflammatory response. Similar effects were observed in mice after exposure to stainless steel welding fumes (Zeidler-Erdely et al., 2011). It is worth noting that the ten cytokines induced by MF-WF or PEPs exposures were most related to asthma and chronic obstructive pulmonary disease (Barnes 2008). A previous study reported that FGF-2 contributes to the progression of pulmonary hypertension in humans and rodents (Izikki et al., 2009). Thus, these results indicated that exposure to ENMs might induce lung diseases, but larger studies are needed to reveal the potential disease risk by the exposure.

Exposure to ENMs also generated oxidative stress, as evidenced from the intracellular generation of ROS and up-regulation of *HO-1* expression (Figure 2B and C). This is in agreement with previous studies that reported WF (Antonini et al., 1999), TiO<sub>2</sub> (Shrivastava et al., 2014), and CuO (Wang et al., 2012) capable of generation intracellular ROS. It is worth mentioning that ROS may lead to epigenetic changes that affect the genome by causing alterations in DNA methylation patterns (Gong et al., 2010).

Environmental stressors, independently of their mode of action (geno- or non-genotoxic), have been shown to target the cellular epigenome and DNA methylation, particularly. Exposure to various sources of particulate matter has been frequently associated with alterations in DNA methylation and TEs in particular (Baccarelli et al., 2009; Madrigano et al., 2011; Miousse et al., 2014a; Salam et al., 2012; Stocco et al., 2013; Tarantini et al., 2009). Loss of TEs-associated DNA methylation is associated with numerous disease, including cancer (Miousse and Koturbash, 2015) and has been also reported early after exposure to both physical and chemical carcinogens (Koturbash et al., 2011b; Miousse et al., 2014b). On the other hand, hypermethylation of TEs have been associated with allergen sensitization, suggesting their involvement in the pathogenesis of asthma and allergies (Sordillo et al., 2013). In the current study, levels of global and TE-associated DNA methylation were not greatly affected by ENMs exposure. This can be possibly explained by the short post-exposure time when a sufficient number of cell divisions had not occurred in order to detect potential alterations in DNA methylation. The observed loss of DNA methyltransferases activity, if sustained, will possibly lead to global genomic hypomethylation. Studies, investigating DNA methylation at later time-points after several cell divisions, will address this issue and are currently in progress in our laboratories.

In contrast to methylation, expression of TEs was greatly affected by exposure to ENMs. This well agrees with other studies, reporting reactivation of L1 and *Alu*/SINEs shortly after exposure to environmental toxicants and carcinogens both in-vitro and in-vivo (Koturbash et al., 2011b; Rudin and Thompson 2001). Reactivation of TEs may result in their retrotransposition via a “copy-and-paste” mechanism, by which a copy of a newly created TE is being introduced elsewhere in the genome, while the “original” remains at its primary location. Such events may have detrimental effects over genomes, by the mean of genome amplification and mutations within the target-genes of retrotransposition. Growing evidence indicates deleterious effects of retrotransposition in human cancers, including lung cancer (Iskow et al., 2010), and retrotransposition stimulated by exposure to various environmental stressors (Terasaki et al., 2013). Despite the significant increase in L1 and *Alu*/SINEs mRNA transcripts, no increases in TEs copy numbers were detected, suggesting absence of

retrotransposition events associated with exposure to ENMs. It is possible that a 24 h time-point is not sufficient to initiate detectable rates of retrotransposition. Indeed, the most recent study indicates that L1 mobilization may take ~ 120 h after exposure (Terasaki et al., 2013).

Accumulating evidence clearly demonstrates the potential of epigenetic parameters to be introduced into risk and safety assessment (Goodman et al., 2010; Herceg et al., 2013; Koturbash et al., 2011a). This study provides a comprehensive characterization of the short-term effects of in-vitro exposure of inhaled ENMs on DNA methylation and DNA methylation machinery. We show that such parameters as expression of TEs and DNA methyltransferases can be further utilized in the characterization of ENMs with the potential to be introduced into safety and risk assessment of ENMs. This study also provides a roadmap for future studies on epigenetic effects of ENMs, including evaluation of longer terms of exposure, involvement of histone modifications, and utilization of in-vivo models, which are ongoing studies in our laboratories. Further delineation of epigenetic alterations caused by ENMs will aid in understanding of the molecular mechanisms of potential health effects associated with exposures.

## Conclusions

In this manuscript, we performed an extensive in-vitro characterization of epigenetic effects associated with DNA methylation by various sources of real world ENMs at low cytotoxic levels. We show that exposure to ENMs modestly affect DNA methylation within the most abundant TEs, but selectively enhance their transcription and suppress the expression of DNA methylation machinery at doses below cytotoxicity. Observed epigenetic alterations are associated with the development of human pathologies, including allergies, asthma, and lung cancer. Further studies are clearly needed in order to investigate short and long-term effects of exposure to ENMs and possible health outcomes of such exposures.

## Supplementary Material

Refer to Web version on PubMed Central for supplementary material.

## Acknowledgments

We would like to thank Dilpreet Singh for his assistance in TEM analysis, Oleksandra Pavliv for her assistance with DNA methylation analysis, Dr. Andrea Baccarelli and Jia Zhong for their help in reviewing the epigenetic results. We are thankful to Dr. Rebecca Helm for editing the manuscript.

This work was supported by the funding from NIEHS Center (Grant# ES-000002), NIOSH, CPSC (Grant # 212-2012-M-51174), NIH UL1TR000039 and KL2TR000063, and the Arkansas Biosciences Institute.

## References

- Antonini JM, Lawryk NJ, Murthy GG, Brain JD. Effect of welding fume solubility on lung macrophage viability and function in vitro. *J Toxicol Environ Health A*. 1999; 58:343–363. [PubMed: 10580758]
- Baccarelli A, Wright RO, Bollati V, Tarantini L, Litonjua AA, Suh HH, et al. Rapid DNA methylation changes after exposure to traffic particles. *Am J Respir Crit Care Med*. 2009; 179:572–578. [PubMed: 19136372]

- Badding MA, Fix NR, Antonini JM, Leonard SS. A comparison of cytotoxicity and oxidative stress from welding fumes generated with a new nickel-, copper-based consumable versus mild and stainless steel-based welding in RAW 264.7 mouse macrophages. *PLoS One*. 2014; 9:e101310. [PubMed: 24977413]
- Balansky R, Longobardi M, Ganchev G, Ilcheva M, Nedyalkov N, Atanasov P, et al. Transplacental clastogenic and epigenetic effects of gold nanoparticles in mice. *Mutat Res*. 2013;751–752. 42–48.
- Barnes PJ. The cytokine network in asthma and chronic obstructive pulmonary disease. *J Clin Invest*. 2008; 118:3546–3556. [PubMed: 18982161]
- Bedran TB, Mayer MP, Spolidorio DP, Grenier D. Synergistic anti-inflammatory activity of the antimicrobial peptides human beta-defensin-3 (hBD-3) and cathelicidin (LL-37) in a three-dimensional co-culture model of gingival epithelial cells and fibroblasts. *PLoS One*. 2014; 9:e106766. [PubMed: 25187958]
- Bollati V, Baccarelli A. Environmental epigenetics. *Heredity (Edinb)*. 2010; 105:105–112. [PubMed: 20179736]
- Choi AO, Brown SE, Szyf M, Maysinger D. Quantum dot-induced epigenetic and genotoxic changes in human breast cancer cells. *J Mol Med (Berl)*. 2008; 86:291–302. [PubMed: 17965848]
- Cohen J, Deloid G, Pyrgiotakis G, Demokritou P. Interactions of engineered nanomaterials in physiological media and implications for in vitro dosimetry. *Nanotoxicology*. 2013; 7:417–431. [PubMed: 22393878]
- Cohen JM, Derk R, Wang L, Godleski J, Kobzik L, Brain J, et al. Tracking translocation of industrially relevant engineered nanomaterials (ENMs) across alveolar epithelial monolayers in vitro. *Nanotoxicology*. 2014a; 8(Suppl 1):216–225. [PubMed: 24479615]
- Cohen JM, Teeguarden JG, Demokritou P. An integrated approach for the in vitro dosimetry of engineered nanomaterials. *Part Fibre Toxicol*. 2014b; 11:20. [PubMed: 24885440]
- de Koning AP, Gu W, Castoe TA, Batzer MA, Pollock DD. Repetitive elements may comprise over two-thirds of the human genome. *PLoS Genet*. 2011; 7:e1002384. [PubMed: 22144907]
- Deloid G, Cohen JM, Darrah T, Derk R, Rojanasakul L, Pyrgiotakis G, et al. Estimating the effective density of engineered nanomaterials for in vitro dosimetry. *Nat Commun*. 2014; 5:3514. [PubMed: 24675174]
- Egli A, Santer DM, O'Shea D, Barakat K, Syedbasha M, Vollmer M, et al. IL-28B is a Key Regulator of B- and T-Cell Vaccine Responses against Influenza. *PLoS Pathog*. 2014; 10:e1004556. [PubMed: 25503988]
- Gong C, Tao G, Yang L, Liu J, Liu Q, Zhuang Z. SiO<sub>2</sub> nanoparticles induce global genomic hypomethylation in HaCaT cells. *Biochem Biophys Res Commun*. 2010; 397:397–400. [PubMed: 20501321]
- Goodman JI, Augustine KA, Cunningham ML, Dixon D, Dragan YP, Falls JG, et al. What do we need to know prior to thinking about incorporating an epigenetic evaluation into safety assessments? *Toxicol Sci*. 2010; 116:375–381. [PubMed: 20430866]
- Halappanavar S, Jackson P, Williams A, Jensen KA, Hougaard KS, Vogel U, et al. Pulmonary response to surface-coated nanotitanium dioxide particles includes induction of acute phase response genes, inflammatory cascades, and changes in microRNAs: a toxicogenomic study. *Environ Mol Mutagen*. 2011; 52:425–439. [PubMed: 21259345]
- Herceg Z, Lambert MP, van VK, Demetriou C, Vineis P, Smith MT, et al. Towards incorporating epigenetic mechanisms into carcinogen identification and evaluation. *Carcinogenesis*. 2013; 34:1955–1967. [PubMed: 23749751]
- Hiraiwa K, van Eeden SF. Contribution of lung macrophages to the inflammatory responses induced by exposure to air pollutants. *Mediators Inflamm*. 2013; 2013:619523. [PubMed: 24058272]
- Iskow RC, McCabe MT, Mills RE, Torene S, Pittard WS, Neuwald AF, et al. Natural mutagenesis of human genomes by endogenous retrotransposons. *Cell*. 2010; 141:1253–1261. [PubMed: 20603005]
- Izikki M, Guignabert C, Fadel E, Humbert M, Tu L, Ziadigie P, et al. Endothelial-derived FGF2 contributes to the progression of pulmonary hypertension in humans and rodents. *J Clin Invest*. 2009; 119:512–523. [PubMed: 19197140]

- James SJ, Melnyk S, Jernigan S, Pavliv O, Trusty T, Lehman S, et al. A functional polymorphism in the reduced folate carrier gene and DNA hypomethylation in mothers of children with autism. *Am J Med Genet B Neuropsychiatr Genet*. 2010; 153B:1209–1220. [PubMed: 20468076]
- Jones PA. Functions of DNA methylation: islands, start sites, gene bodies and beyond. *Nat Rev Genet*. 2012; 13:484–492. [PubMed: 22641018]
- Kohli RM, Zhang Y. TET enzymes, TDG and the dynamics of DNA demethylation. *Nature*. 2013; 502:472–479. [PubMed: 24153300]
- Koturbash I, Beland FA, Pogribny IP. Role of epigenetic events in chemical carcinogenesis--a justification for incorporating epigenetic evaluations in cancer risk assessment. *Toxicol Mech Methods*. 2011a; 21:289–297. [PubMed: 21495867]
- Koturbash I, Scherhag A, Sorrentino J, Sexton K, Bodnar W, Tryndyak V, et al. Epigenetic alterations in liver of C57BL/6J mice after short-term inhalational exposure to 1,3-butadiene. *Environ Health Perspect*. 2011b; 119:635–640. [PubMed: 21147608]
- Lee YH, Cheng FY, Chiu HW, Tsai JC, Fang CY, Chen CW, et al. Cytotoxicity, oxidative stress, apoptosis and the autophagic effects of silver nanoparticles in mouse embryonic fibroblasts. *Biomaterials*. 2014; 35:4706–4715. [PubMed: 24630838]
- Li S, Wang H, Qi Y, Tu J, Bai Y, Tian T, et al. Assessment of nanomaterial cytotoxicity with SOLiD sequencing-based microRNA expression profiling. *Biomaterials*. 2011; 32:9021–9030. [PubMed: 21889204]
- Madrigano J, Baccarelli A, Mittleman MA, Wright RO, Sparrow D, Vokonas PS, et al. Prolonged exposure to particulate pollution, genes associated with glutathione pathways, and DNA methylation in a cohort of older men. *Environ Health Perspect*. 2011; 119:977–982. [PubMed: 21385671]
- Miousse IR, Chalbot MC, Aykin-Burns N, Wang X, Basnakian A, Kavouras IG, et al. Epigenetic alterations induced by ambient particulate matter in mouse macrophages. *Environ Mol Mutagen*. 2014a; 55:428–435. [PubMed: 24535919]
- Miousse IR, Shao L, Chang J, Feng W, Wang Y, Allen AR, et al. Exposure to low-dose (56)Fe-ion radiation induces long-term epigenetic alterations in mouse bone marrow hematopoietic progenitor and stem cells. *Radiat Res*. 2014b; 182:92–101. [PubMed: 24960414]
- Miousse IR, Koturbash I. The fine LINE: methylation drawing the cancer landscape. *Biomed Res Int*. 2015 In Press.
- Ng CT, Dheen ST, Yip WC, Ong CN, Bay BH, Lanry Yung LY. The induction of epigenetic regulation of PROS1 gene in lung fibroblasts by gold nanoparticles and implications for potential lung injury. *Biomaterials*. 2011; 32:7609–7615. [PubMed: 21764123]
- Pirela SV, Pyrgiotakis G, Bello D, Thomas T, Castranova V, Demokritou P. Development and characterization of an exposure platform suitable for physico-chemical, morphological and toxicological characterization of printer-emitted particles (PEPs). *Inhal Toxicol*. 2014a; 26:400–408. [PubMed: 24862974]
- Pirela SV, Sotiriou GA, Bello D, Shafer M, Bunker KL, Castranova V, et al. Consumer exposures to laser printer-emitted engineered nanoparticles: A case study of life-cycle implications from nano-enabled products. *Nanotoxicology* Nov. 2014b; 11:1–9. Epub ahead of print.
- Pyrgiotakis G, McDevitt J, Gao Y, Branco A, Eleftheriadou M, Lemos B, et al. Mycobacteria inactivation using Engineered Water Nanostructures (EWNS). *Nanomedicine*. 2014; 10:1175–1183. [PubMed: 24632246]
- Rudin CM, Thompson CB. Transcriptional activation of short interspersed elements by DNA-damaging agents. *Genes Chromosomes Cancer*. 2001; 30:64–71. [PubMed: 11107177]
- Salam MT, Byun HM, Lurmann F, Breton CV, Wang X, Eckel SP, et al. Genetic and epigenetic variations in inducible nitric oxide synthase promoter, particulate pollution, and exhaled nitric oxide levels in children. *J Allergy Clin Immunol*. 2012; 129:232–239. [PubMed: 22055874]
- Schmittgen TD, Livak KJ. Analyzing real-time PCR data by the comparative C(T) method. *Nat Protoc*. 2008; 3:1101–1108. [PubMed: 18546601]
- Setyawati MI, Tay CY, Chia SL, Goh SL, Fang W, Neo MJ, et al. Titanium dioxide nanomaterials cause endothelial cell leakiness by disrupting the homophilic interaction of VE-cadherin. *Nat Commun*. 2013; 4:1673. [PubMed: 23575677]



- Shrivastava R, Raza S, Yadav A, Kushwaha P, Flora SJ. Effects of sub-acute exposure to TiO<sub>2</sub>, ZnO and Al<sub>2</sub>O<sub>3</sub> nanoparticles on oxidative stress and histological changes in mouse liver and brain. *Drug Chem Toxicol*. 2014; 37:336–347. [PubMed: 24344737]
- Sisler JD, Pirela SV, Friend S, Farcas M, Schwegler-Berry D, Shvedova A, et al. Small airway epithelial cells exposure to printer-emitted engineered nanoparticles induces cellular effects on human microvascular endothelial cells in an alveolar-capillary co-culture model. *Nanotoxicology*. Nov. 2014; 1:1–11. Epub ahead of print.
- Sordillo JE, Lange NE, Tarantini L, Bollati V, Zanobetti A, Sparrow D, et al. Allergen sensitization is associated with increased DNA methylation in older men. *Int Arch Allergy Immunol*. 2013; 161:37–43. [PubMed: 23257623]
- Sotiriou GA, Diaz E, Long MS, Godleski J, Brain J, Pratsinis SE, et al. A novel platform for pulmonary and cardiovascular toxicological characterization of inhaled engineered nanomaterials. *Nanotoxicology*. 2012; 6:680–690. [PubMed: 21809902]
- Sotiriou GA, Watson C, Murdaugh KM, Darrah TH, Pyrgiotakis G, Elder A, et al. Engineering safer-by-design, transparent, silica-coated ZnO nanorods with reduced DNA damage potential. *Environ Sci Nano*. 2014; 1:144–153. [PubMed: 24955241]
- Stocco A, Karlsson HL, Coppede F, Migliore L. Epigenetic effects of nano-sized materials. *Toxicology*. 2013; 313:3–14. [PubMed: 23238276]
- Tarantini L, Bonzini M, Apostoli P, Pegoraro V, Bollati V, Marinelli B, et al. Effects of particulate matter on genomic DNA methylation content and iNOS promoter methylation. *Environ Health Perspect*. 2009; 117:217–222. [PubMed: 19270791]
- Terasaki N, Goodier JL, Cheung LE, Wang YJ, Kajikawa M, Kazazian HH Jr, et al. In vitro screening for compounds that enhance human L1 mobilization. *PLoS One*. 2013; 8:e74629. [PubMed: 24040300]
- Wang Z, Li N, Zhao J, White JC, Qu P, Xing B. CuO nanoparticle interaction with human epithelial cells: cellular uptake, location, export, and genotoxicity. *Chem Res Toxicol*. 2012; 25:1512–1521. [PubMed: 22686560]
- Watson C, Ge J, Cohen J, Pyrgiotakis G, Engelward BP, Demokritou P. High-throughput screening platform for engineered nanoparticle-mediated genotoxicity using CometChip technology. *ACS Nano*. 2014; 8:2118–2133. [PubMed: 24617523]
- Xia T, Hamilton RF, Bonner JC, Crandall ED, Elder A, Fazlollahi F, et al. Interlaboratory evaluation of in vitro cytotoxicity and inflammatory responses to engineered nanomaterials: the NIEHS Nano GO Consortium. *Environ Health Perspect*. 2013; 121:683–690. [PubMed: 23649538]
- Xiong S, Tang Y, Ng HS, Zhao X, Jiang Z, Chen Z, et al. Specific surface area of titanium dioxide (TiO<sub>2</sub>) particles influences cyto- and photo-toxicity. *Toxicology*. 2013; 304:132–140. [PubMed: 23295712]
- Zeidler-Erdely PC, Kashon ML, Li S, Antonini JM. Response of the mouse lung transcriptome to welding fume: effects of stainless and mild steel fumes on lung gene expression in A/J and C57BL/6J mice. *Respir Res*. 2010; 11:70. [PubMed: 20525249]
- Zeidler-Erdely PC, Battelli LA, Stone S, Chen BT, Frazer DG, Young SH, et al. Short-term inhalation of stainless steel welding fume causes sustained lung toxicity but no tumorigenesis in lung tumor susceptible A/J mice. *Inhal Toxicol*. 2011; 23:112–120. [PubMed: 21309664]

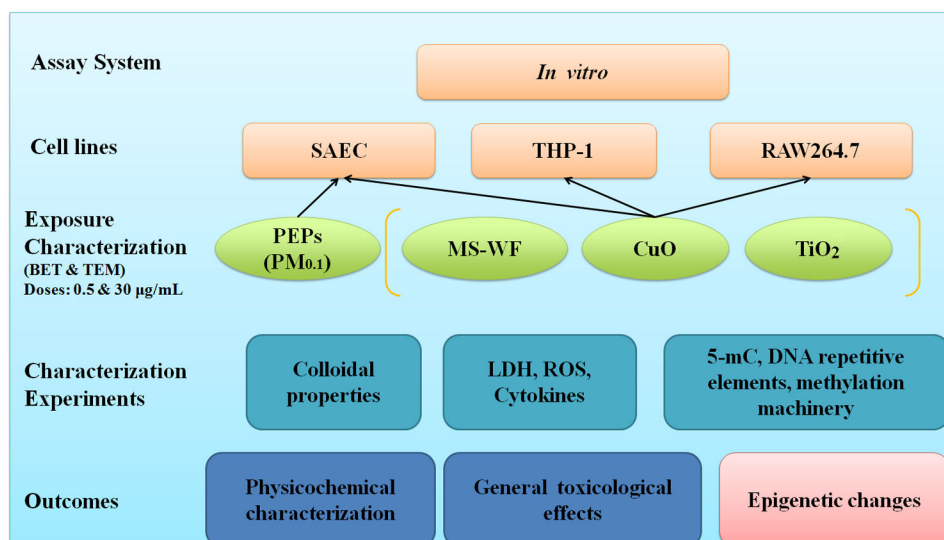


Figure 1.

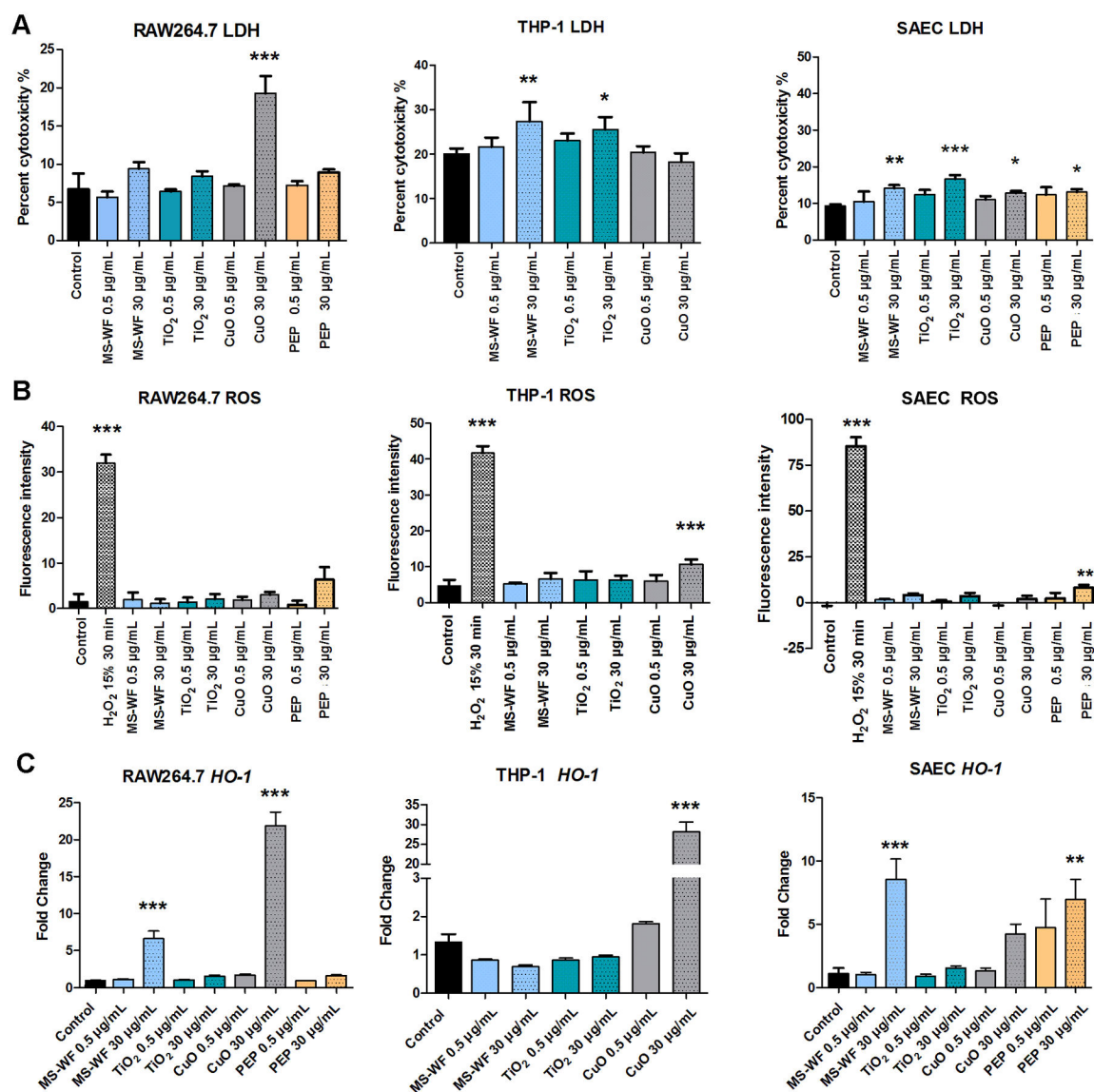


Figure 2.

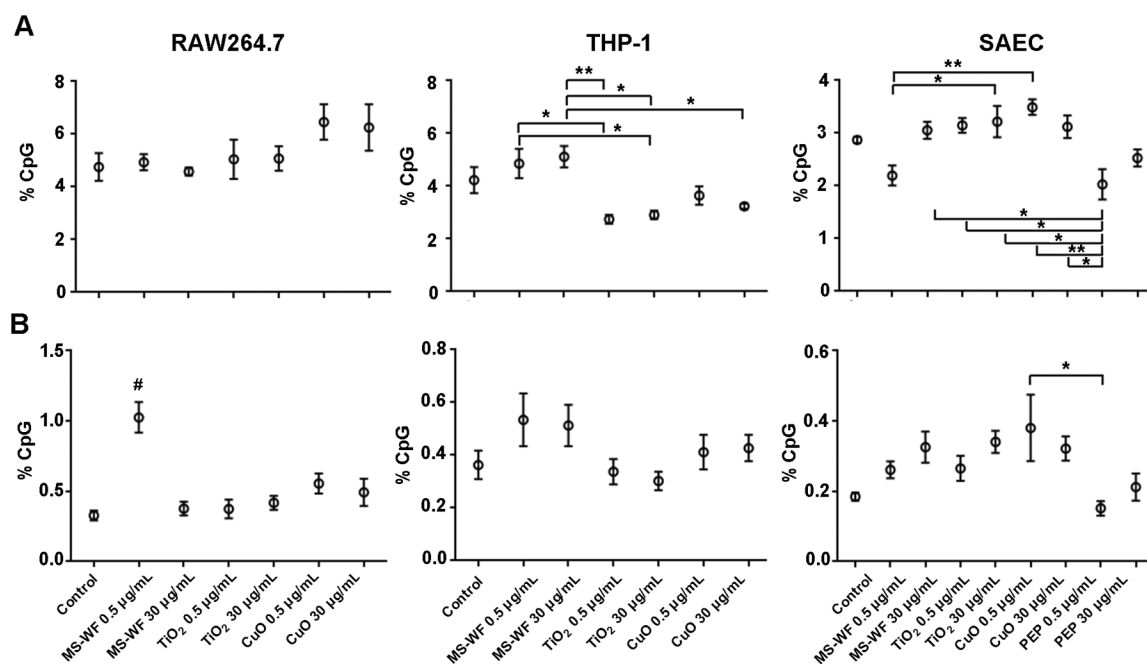


Figure 3.

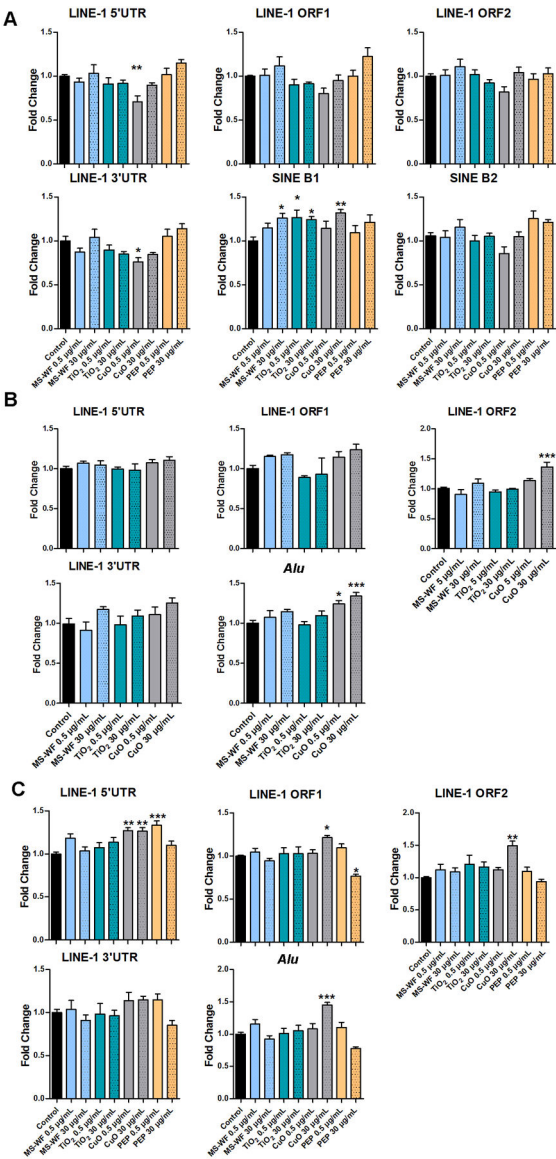


Figure 4.

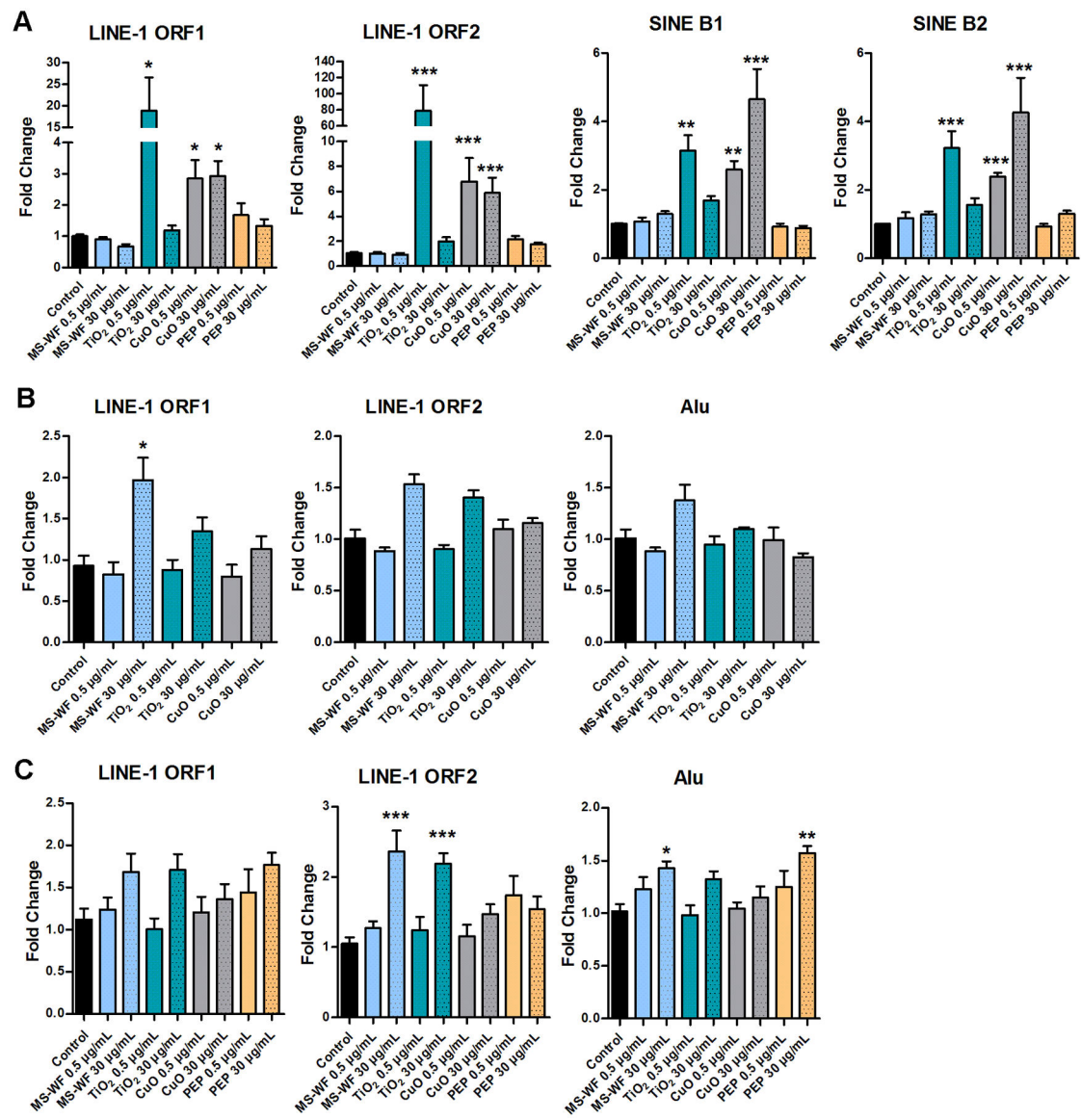


Figure 5.



